Oxidation Behavior of Nanocrystalline Cu-Si Alloys Prepared by Mechanical Alloying

Y. Su, G. Y. Fu*, Q. Liu

College of Mechanical Engineering, Shenyang Institute of Chemical Technology, 110142 Shenyang (China)

(Received March 29, 2009)

ABSTRACT

The oxidation of two Cu-Si alloys with different compositions prepared by conventional casting (CA) and mechanical alloying (MA) at 973 and 1073 K under 1 atm of flowing pure O_2 was conducted to investigate the influence of grain size on the high-temperature oxidation resistance of alloys by TGA, SEM and XRD. The results show that CA Cu-0.1Si alloy at both temperatures, MA Cu-0.1Si alloy at 1073 K in previous 23 h, CA Cu-0.5Si alloy at 1073 K and MA Cu-0.5Si alloy at 973 K obey the parabolic law, and on the whole the mass gain of MA alloys is smaller than that of the corresponding CA alloys. The analysis of oxide scales shows that all alloys did not form continuous layers of SiO_2 but formed complex and similar scales after oxidation, which involved layers composed of mixed oxides of Cu_2O and SiO_2 rich in SiO_2 acting as barriers to restrain further diffusion of both copper and oxygen. The reduction in the alloy grain size speeds up the diffusion of the reactive component of Si, improves the volume fraction of SiO_2 in the mixed oxides of Cu_2O and SiO_2, and improves the high- temperature oxidation resistance of Cu-Si alloys.

Key Words: nanocrystalline, grain refinement, oxidation, Cu-Si alloy, mechanical alloying

1. INTRODUCTION

The oxidation resistance of alloys depends on the selective oxidation of reactive elements forming stable and slowly growing protective oxides such as Al_2O_3, Cr_2O_3 and SiO_2. The formation of protective scales can be realized by increasing the contents of Si, Cr or Al, while this generally has an adverse effect on the mechanical properties of alloys /1-2/.

Nanostructured materials, whose grain sizes are in the range of 1-100 nm, have recently been attracting the attention of material scientists, physicists and chemists, due to their superior mechanical, physical and chemical properties. Extensive studies on the oxidation behaviors of nanocrystalline high-temperature alloys have been performed by many researchers /3-7/. And it is evident that nanocrystallization can enhance the selective oxidation for many alloys and reduce the critical concentration of Si, Cr or Al needed to form the stable and slowly growing protective oxides, so the contradiction of mechanical properties and oxidation resistance of alloys can possibly be solved.

Copper has been widely used in VLSI and many engineering fields for its high electric and thermal conductivity and good plasticity /8-9/, while the poor oxidation resistance limits its applications at high temperatures /10-12/. Protecting copper or Cu-base alloys from oxidation is therefore critical. In recent

* Correspondent: guangyan. fu@gmail.com (Dr. G. Y. Fu)

years, a lot of papers have been published about the additions of Cr and/or Al to Cu or Cu-base alloys /8,13-17/. However, there have been few studies on the high-temperature oxidation of Cu-Si alloys, especially on nanocrystalline Cu-Si alloys.

The purpose of this paper is to study the influence of grain size on the high-temperature oxidation resistance of Cu-Si alloys. All alloys with two compositions (Cu-0.1Si and Cu- 0.5Si, mass fraction) were prepared by different techniques of conventional casting (CA) and mechanical alloying (MA), which result in differences in microstructure, especially in grain size.

2. EXPERIMENTAL

CA: Cu-Si alloys with nominal compositions (mass fraction) of Cu-0.1Si and Cu-0.5Si were prepared from high-purity metals by repeated arc-melting under a Ti-gettered argon atmosphere using non-consumable tungsten electrodes from appropriate amounts of pure Cu (purity> 99.8%) and Si (purity> 99.9%). The alloy ingots were subsequently annealed in an argon atmosphere at 1073 K for 24 h to remove the residual mechanical stresses and to achieve a better equilibration of the alloy. The actual average composition (mass fraction) of the CA alloys is Cu-0.13Si and Cu-0.55Si respectively.

MA: Cu-0.1Si and MA Cu-0.5Si alloys were prepared as follows. Elemental copper (purity> 99.8%) and silicon powders (purity> 99.9%) with particle size of about 100 μm were blended according to the Cu to Si mass ratio. Mechanical alloying was carried out in a QM-1SP4 planetary miller. Two powders were first stir-mixed in stainless steel vials with hardened GCr15 steel balls, and the ball to powder mass ratio was about 10:1. Each vial with powders was evacuated to about 10 Pa and then filled with pure argon. During ball milling with a speed of 180 rpm a relay was used to control intermediate stops of 30 min every hour to avoid excessive heat effect. The whole powders were prepared by mechanical alloying for 100 h in order to obtain alloying on atomic level. Nearly fully dense samples were prepared by hot pressing at 1253 K for 10 min and the pressure of 64 MPa in vacuum of 0.03 Pa using a graphite die with inner diameter of 20 mm.

Finally, the resulting ingots were annealed for 12 h at 1073 K to stabilize the grain structure and relieve mechanical stresses induced by hot pressing. The density of MA samples was measured using Archimedes method, then the theoretical density and porosity were calculated, all of which were listed in Table 1. The actual average composition (mass fraction) of the MA alloys is Cu-0.15Si and Cu-0.6Si respectively.

Table 1

Density and porosity of MA Cu-Si alloys

Alloy	Theoretical Density ($g \cdot cm^{-3}$)	Measured Density ($g \cdot cm^{-3}$)	Porosity (%)
MA Cu-0.15Si	8.92	8.76	1.79
MA Cu-0.6Si	8.81	8.55	2.95

Figure 1 shows the optical micrographs of CA Cu-Si alloys treated with metallographic etch, from which the grain boundaries are clearly seen and the difference in color between different grains is revealed and through which the grain size can easily be measured, which is about 550 μm in average for both CA Cu-0.1Si and CA Cu-0.5Si alloys. Both MA Cu-0.1Si and MA Cu-0.5Si alloys were analyzed by X-ray diffraction. A measurement of the average grain size by using the Scherrer Formula gave a value of about 50 nm of each MA alloy, which was within the nanosize range. So the technique of MA compared with CA has greatly reduced the grain size of Cu-Si alloys.

Flat specimens with dimensions of 8 mm×8 mm×1.5 mm were cut from the ingots by wire cutting. After drilling a hole of 1 mm diameter near the edge, every slice was ground down to 800-grit SiC paper, washed in water, alcohol and acetone and then dried immediately before use. Before oxidation, every specimen was suspended with a platinum wire.

Isothermal oxidation tests were conducted under 1 atm of flowing pure O_2 at 973 and 1073 K for 24 h using thermogravimetric analyzer (TGA, Zry-2P model), which includes a vertical tube furnace. After reaching the reaction temperature, the vertical furnace was raised to locate the specimen in the hot zone. The

weight changes were measured continuously at both temperatures and recorded by a computer. After oxidation for 24 h, the samples were cooled to room temperature in the furnace. Then the oxidized samples were analyzed by X-ray diffraction (XRD) and a scanning electron microscope (SEM) equipped with an energy-dispersive X-ray spectrometer attachment (EDX).

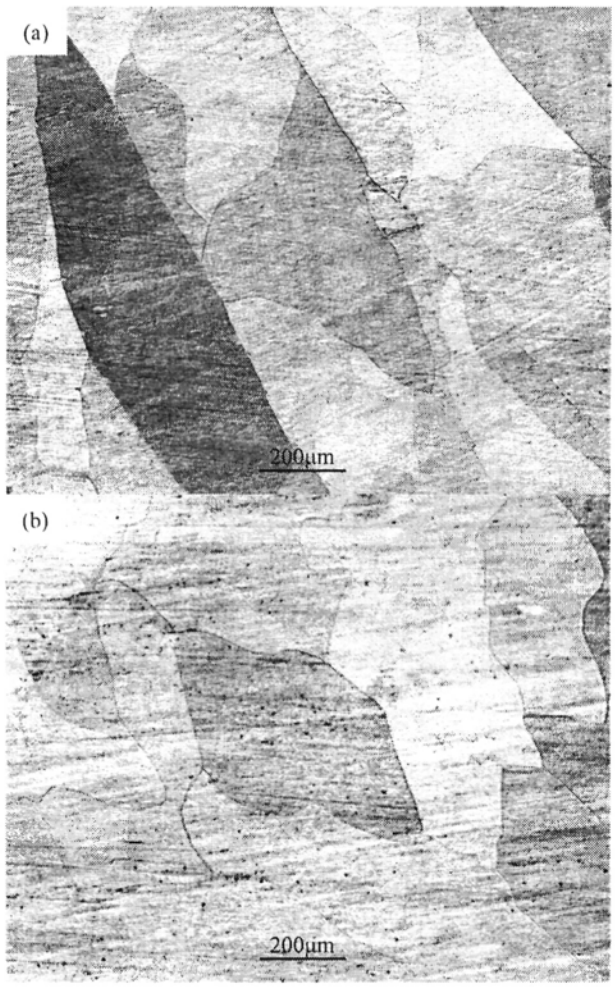

Fig. 1: Optical micrographs of CA Cu-Si alloys (a) Cu-0.1Si and (b) Cu-0.5Si

3. RESULTS

3.1 Oxidation kinetics

Figure 2 shows the oxidation curves using mass gain per unit area vs. time. The curves were obtained for Cu-0.1Si and Cu-0.5Si alloys prepared by different techniques oxidized continuously under 1 atm of flowing pure O_2 at 973 and 1073 K for 24 h. It can be seen that the mass gain of Cu-Si alloys with the same composition prepared by the same technique increases when temperature increases. The square of the specific mass gain as a function of oxidation time for some Cu-Si alloys is shown in Fig. 3. It can be seen that the plots of the square of mass gain of CA Cu-0.1Si alloy at both temperatures, MA Cu-0.1Si alloy at 1073 K in previous 23 h, CA Cu-0.5Si alloy at 1073 K and MA Cu-0.5Si alloy at 973 K result in straight lines, indicating that the oxidation kinetics of them follow a parabolic oxidation law. The data of the approximate parabolic rate constants (K_p) can be derived from Fig. 3 using linear regression analysis method, and the results are listed in Table 2.

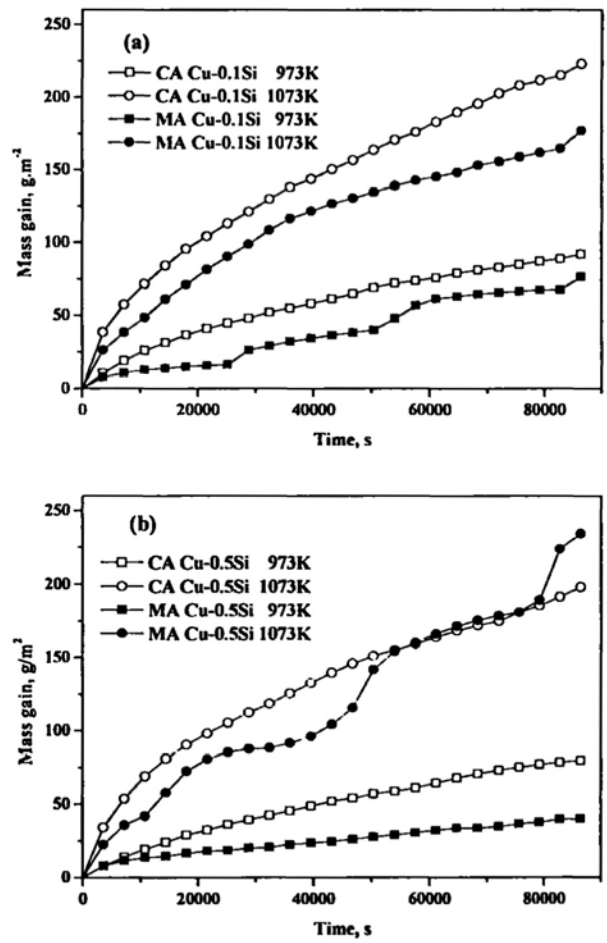

Fig. 2: Curves of oxidation kinetics of CA and MA Cu-Si alloys at 973 and 1073 K under 1 atm of O_2 (a) Cu-0.1Si and (b) Cu-0.5Si

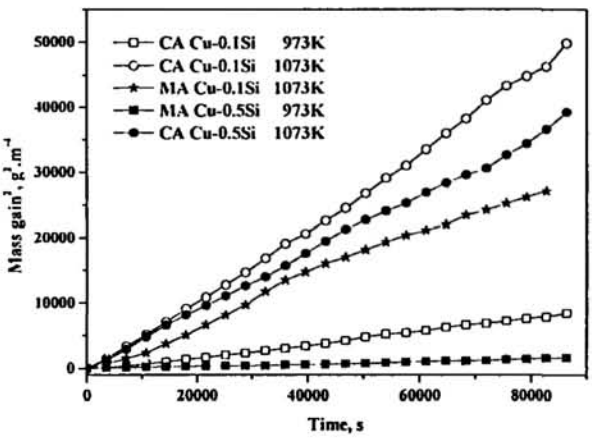

Fig. 3: Square of mass gain vs. time curves of Cu-Si alloys oxidized under 1 atm of O_2 for 24 h

Table 2

Approximate parabolic rate constants (K_p) for the oxidation of Cu-Si alloys oxidized under 1 atm of O_2

Alloy	Temperature (K)	K_p ($g^2 \cdot m^{-4} \cdot s^{-1}$)
CA Cu-0.1Si	973	9.38×10^{-2}
CA Cu-0.1Si	1073	5.53×10^{-1}
MA Cu-0.1Si	1073	3.42×10^{-1}
CA Cu-0.5Si	1073	4.40×10^{-1}
MA Cu-0.5Si	700	1.67×10^{-2}

In Fig. 2a, the two oxidation curves above are of CA and MA Cu-0.1Si alloys oxidized at 1073 K. From Table 2, the parabolic rate constant of MA Cu-0.1Si alloy is 3.42×10^{-1} $g^2 \cdot m^{-4} \cdot s^{-1}$, which is smaller than that of CA Cu-0.1Si alloy (5.53×10^{-1} $g^2 \cdot m^{-4} \cdot s^{-1}$). The two oxidation curves below are of CA and MA Cu-0.1Si alloys oxidized at 973 K. It can be seen that the curve of MA Cu-0.1Si alloy is very irregular, indicating abnormal oxidation occurs. In spite of this, it is clear that the mass gain of MA Cu-0.1Si alloy is smaller than that of CA Cu-0.1Si alloy.

In Fig. 2b, it can also be seen that at 973 K the mass gain of MA Cu-0.5Si alloy is smaller than that of CA Cu-0.5Si alloy. At 1073 K, similar to MA Cu-0.1Si alloy at 973 K, the curve of MA Cu-0.5Si alloy is also irregular. In initial 15 h, the mass gain of MA Cu-0.5Si alloy is smaller than that of CA Cu-0.5Si. From 15 to 22 h, the mass gain of them is almost equal, while at the last 2 h, the mass gain of MA Cu-0.5Si alloy increases suddenly and exceeds that of CA Cu-0.5Si alloy.

According to the above analysis, though not all alloys oxidized for 24 h obey the parabolic law, and some alloys exhibit abnormal oxidation behavior, it can clearly be seen on the whole that the mass gain of alloys prepared by MA is smaller than that of the corresponding alloys prepared by CA subjected to the same treatment. Mechanical alloying improves the oxidation resistance of Cu-Si alloys.

3.2 Scale microstructure and composition

The microstructures of the oxide scales formed on the surface of the different specimens are shown in Figs. 4-7. In most cases, cracks within the oxide scales and at the metal-oxide interfaces were observed, which formed likely in the oxidation process for the poor adherent of oxide scales to the matrix or during preparation of the cross-sectional samples.

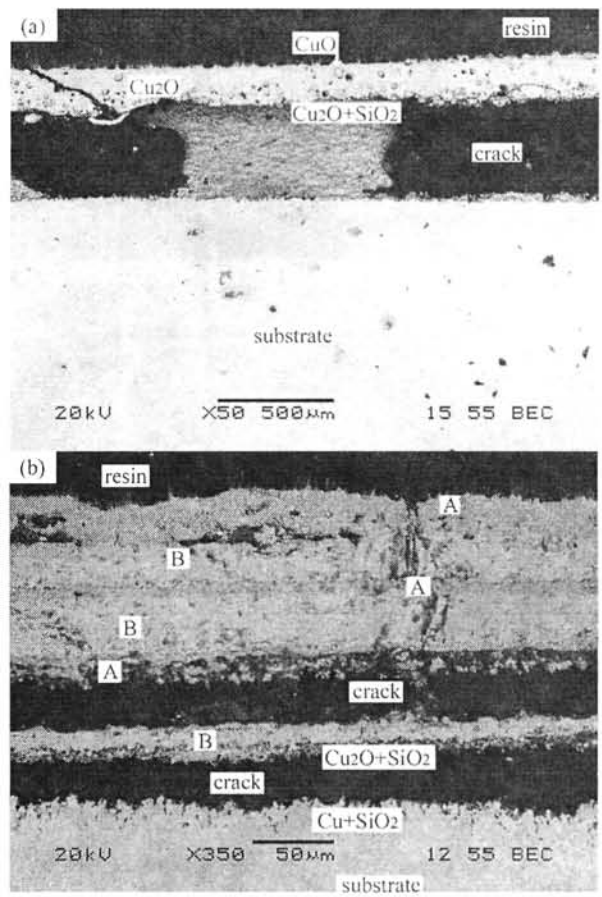

Fig. 4: Cross-sectional morphologies of CA and MA Cu-0.1Si alloys oxidized at 973 K under 1 atm of O2 for 24 h (a) CA Cu-0.1Si and (b) MA Cu-0.1Si

Figure 4 shows the cross-sectional morphologies of CA (a) and MA (b) Cu-0.1Si alloys oxidized at 973 K under 1 atm of O_2 for 24 h. It can be seen from Fig. 4b that the external scales are complex, which involves zones A (dark gray) alternating with zones B (light gray). Compositional analysis by XRD and EDX shows that the dark gray layers are CuO, and the light gray layers are Cu_2O and CuO. The formation of this microstructure is because of the cracks within the oxide scale which allow oxygen to diffuse inward through the oxide scale or even to the scale/matrix interface easily, which is in accordance with its irregular oxidation kinetics shown in Fig. 2a. The zones beneath the dark gray layers alternating with light gray layers are mixed oxides of Cu_2O and SiO_2 rich in SiO_2. In addition, internal oxidation occurred obviously. Fig. 4a shows that CA Cu-0.1Si alloy oxidized at 973 K formed complex scales of $CuO \rightarrow Cu_2O \rightarrow Cu_2O$ and SiO_2 (rich in SiO_2) from outside to inside, and the total thickness of which is thicker than that of MA Cu-0.1Si alloy subjected to the same treatment. It can be seen from Fig. 4a that the internal oxidation is not obvious, maybe because the external scales grow so fast that the thickness of internal oxidation zone is small enough to be neglected.

Figure 5 shows the cross-sectional morphologies of CA (a) and MA (b) Cu-0.1Si alloys oxidized at 1073 K under 1 atm of O_2 for 24 h. The Cu-0.1Si alloys prepared by different techniques formed similar scales after oxidation like CA Cu-0.1Si oxidized at 973 K: $CuO \rightarrow Cu_2O \rightarrow Cu_2O$ and SiO_2 (rich in SiO_2)$\rightarrow$internal oxidation zone. The main difference is that the total thickness of oxide scales formed on MA Cu-0.1Si alloy is also thinner than that of CA Cu-0.1Si alloy subjected to the same treatment.

Figure 6 and Figure 7 show the cross-sectional morphologies of CA and MA Cu-0.5Si alloys oxidized at 973 and 1073 K under 1 atm of O_2 for 24 h. It can be seen from the figures that Cu-0.5Si alloys prepared by different techniques formed similar oxide scales as Cu-0.1Si alloys: $CuO \rightarrow Cu_2O \rightarrow Cu_2O$ and SiO_2 (rich in SiO_2)$\rightarrow$internal oxidation zone, but the total thickness of oxide scale formed on MA Cu-0.5Si alloys is also thinner than that of CA Cu-0.5Si alloy subjected to the same treatment. In Fig. 7b, MA Cu-0.5Si alloy oxidized at 1073 K formed similar oxide scales as MA Cu-0.1Si alloy oxidized at 973 K: dark gray layers (CuO) alternating with light gray layers (Cu_2O + CuO), beneath which mixed oxides of Cu_2O and SiO_2 rich in SiO_2 also formed. This structure is in accordance with its irregular oxidation kinetics shown in Fig. 2b. In addition, internal oxidation also occurred to MA Cu-0.5Si alloy oxidized at 1073 K.

According to the above analysis, although cracks within the oxide scales formed on some MA Cu-Si alloys and even formed complex scales of CuO alternating with Cu_2O and CuO, which had an adverse effect on the oxidation resistance, MA Cu-Si alloys formed thinner oxide scales than CA Cu-Si alloys subjected to the same treatment on the whole, which was in accordance with the higher oxidation rate of CA Cu-Si alloys observed in the TGA measurement. Mechanical alloying improves the oxidation resistance of Cu-Si alloys.

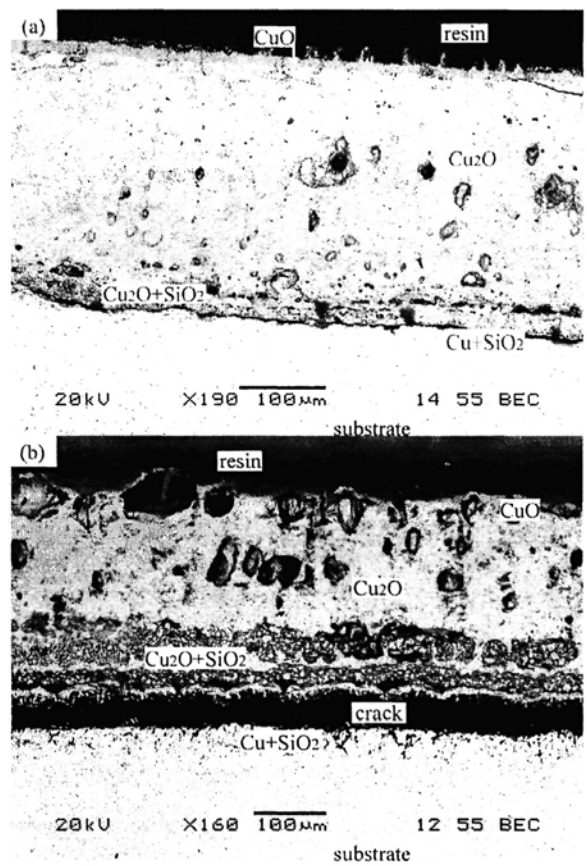

Fig. 5: Cross-sectional morphologies of CA and MA Cu-0.1Si alloys oxidized at 1073 K under 1 atm of O_2 for 24 h (a) CA Cu-0.1Si and (b) MA Cu-0.1Si

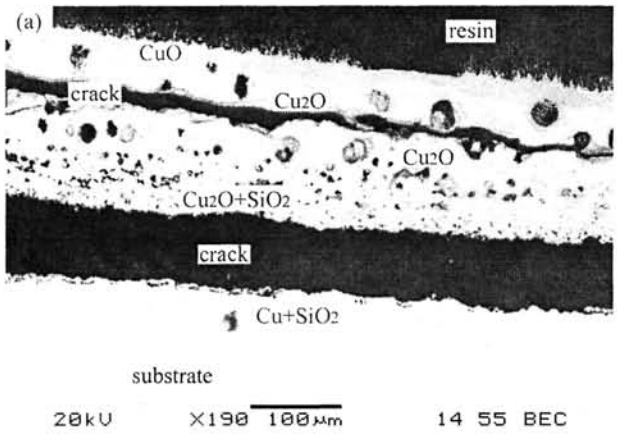

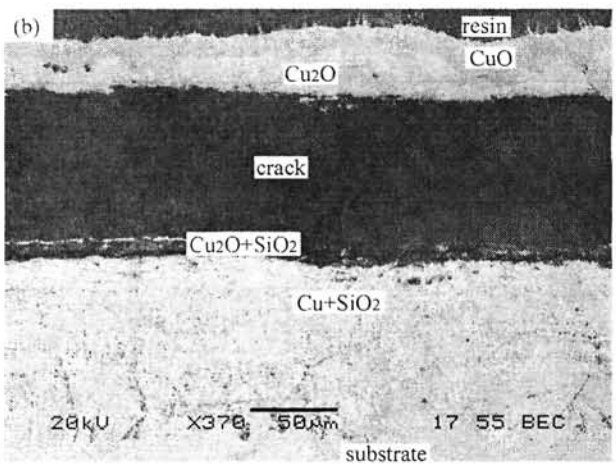

Fig. 6: Cross-sectional morphologies of CA and MA Cu-0.5Si alloys oxidized at 973 K under 1 atm of O_2 for 24 h (a) CA Cu-0.5Si and (b) MA Cu-0.5Si

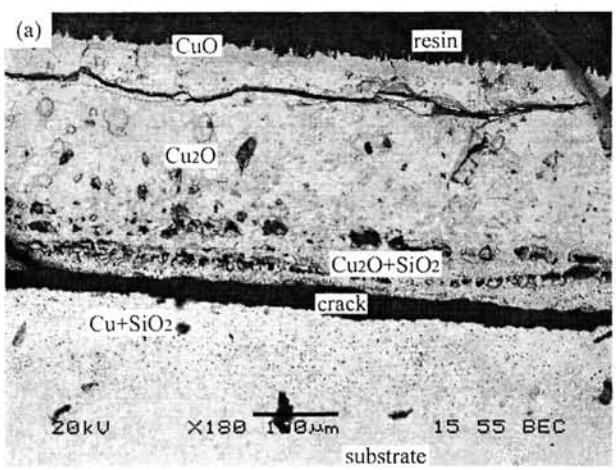

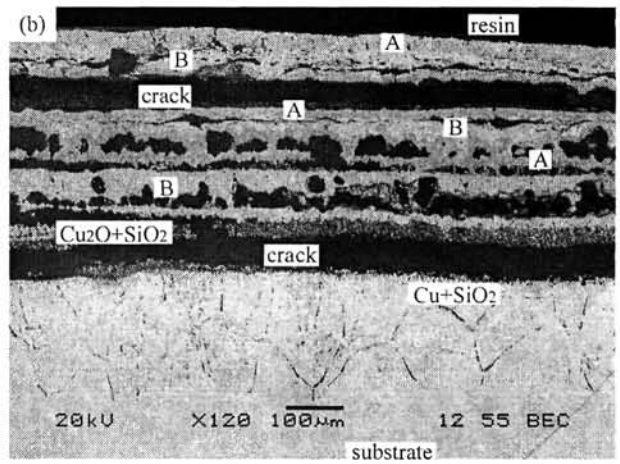

Fig. 7: Cross-sectional morphologies of CA and MA Cu-0.5Si alloys oxidized at 1073 K under 1 atm of O_2 for 24 h (a) CA Cu-0.5Si and (b) MA Cu-0.5Si

4. DISCUSSION

The high-temperature oxidation behaviors of metal/alloy are determined by thermodynamic and dynamic factors. For Cu-Si alloy system, thermodynamically, at high temperature, the stablities of the three various oxides, CuO, Cu_2O and SiO_2, increase in ture /18-19/, therefore Si is the reactive component, while Cu is the noble component. Because the oxygen pressure used in this study is much higher than the equilibrium decomposition pressure, three various oxides may all form when oxidation starts. Kinetically, there are much more differences among the oxidation rates of two components. CuO and Cu_2O grow more rapidly than SiO_2 on the alloy surface. Under ideal conditions, when oxidation starts, CuO, Cu_2O and SiO_2 may form respectively, but CuO and Cu_2O overlays SiO_2 because of the rapid growth rate of copper oxides. Thus, a continuous external scale of CuO forms initially. With the formation of CuO, alloy/scale interface transfers inward, and the oxygen pressure at alloy/scale interface decreases gradually. Then continuous Cu_2O is formed and so is continuous SiO_2. When continuous layer of SiO_2 formed, both the outward diffusion of Cu and the inward diffusion of oxygen are blocked and the oxidation rate becomes

eventually controlled by the growth rate of SiO_2, which is very small, so the Cu-Si alloys are protected from further oxidation. Further investigations indicate that the formation process of continuous SiO_2 is that at the beginning, the SiO_2 grains formed were few, but with the oxidation proceeding and Si diffusing outward to react, more and more SiO_2 grains formed. It became likely for SiO_2 grains to connect with one another to form continuous layer, which was protective for Cu-Si alloys. Based on the analysis above, all factors that are beneficial to promote the formation of SiO_2 and the connection of them to form continuous scale of SiO_2 are likely to improve the high-temperature oxidation resistance of Cu-Si alloys.

In comparison with CA Cu-Si alloys, the microstructure of MA Cu-Si alloys changes a great deal, and these changes have a large impact on their oxidation behavior.

Mechanical alloying can be used to produce materials with extremely fine grain sizes /20-22/, and the most direct effect of the strong reduction of the grain size obtained by this method is the appearance of large concentrations of grain boundaries /23/. As a consequence of their rather open and disorder structure, the grain boundaries allow a faster transport of the components in the alloy in comparison with normal bulk diffusion in the presence of chemical potential gradients /24/. Thus, for fine-grained materials the bulk diffusion coefficient of any given species should be replaced by a corresponding effective-diffusion coefficient, D_{eff} /25/,

$$D_{eff} = (1-f)D_L + fD_B$$

where D_L and D_B are the diffusion coefficients in the lattice and along the grain boundaries respectively, and f is the fraction of the total number of diffusion sites located in the boundaries. Assuming that grains have the shape of spheres or cubes, the volume fraction of interfaces may be estimated as $3\Delta/d$ (where Δ is the average interface thickness and d is the average grain diameter) /26/. If d is very small, then D_{eff} is dominated by the second term on the right side of the equation. The increase in the effective-diffusion coefficient will thus depend on the relative magnitude of D_L and D_B. Typically, the activation energy for short-circuit diffusion is 0.5–0.7 times smaller than that for lattice diffusion, while D_B / D_L is usually in the range of 10^4–10^6 /27/. Consequently, the larger value of D_{eff} as compared to D_B favors the formation of the most stable oxidation. For MA Cu-Si alloys, the reduction of grain size produces large amount of high-diffusivity paths and the ratio D_B / D_L increase. The reactive element of Si diffuses outward more rapidly, so grain refining promotes the formation of continuous and protective scales of SiO_2.

Apart from high diffusivities of the reactants through the MA Cu-Si alloys, the faster transport of the reactants through the scales due to a significant contribution from grain-boundary diffusion can also have great effects on the oxidation. Even though no clear trend or relation has apparently been established between the grain size of the alloy and that of the corresponding scales, the scales growing on fine grain materials also tend to have smaller oxide grains /28/. For MA Cu-Si alloys, this will affect the growth rate of protective scales of SiO_2 by the same mechanism involved in mass transport through the substrate of alloys /29/, as discussed above. Additionally, since the oxide grains formed on nanocrystalline alloys are much smaller than those formed on alloys with normal grain size, there are many more nucleation sites on the nanocrystalline alloys than those on ordinary alloys, so the distribution of SiO_2 grains formed on nanocrystalline Cu-Si alloys is more dispersed and more uniform, and this will be helpful for SiO_2 grains to connect with one another and form continuous scales of SiO_2.

In a word, grain refining promotes the formation of protective scale of SiO_2. In this study, continuous scales of SiO_2 are not observed maybe because the content of Si is too low to favor the formation of them, or maybe because the plasticity of SiO_2 is poor and the scale of SiO_2 is fragmented in the oxidation process, during cooling after oxidation or during the preparation of cross-sectional samples. However, in any specimens after oxidation, mixed oxides of Cu_2O and SiO_2 rich in SiO_2 are found, which can also act as barriers to restrain both the outward diffusion of Cu and the inward diffusion of oxygen effectively. Grain refining promotes the formation of SiO_2, so it can also promote the formation of mixed oxides of Cu_2O and SiO_2 rich in

SiO_2, and at the same time raise the volume fraction of SiO_2 in the mixed oxides so that the blocking function should be more effective, which is the direct reason that mechanical alloying improves the oxidation resistance of Cu-Si alloys.

From another point of view, the effect of grain refining on the oxidation of binary single-phase Cu-Si alloys has two aspects. First, as explained above, grain refining produces more high-diffusivity paths and thereby promotes the diffusion of the reactive element of Si, accelerates the formation of SiO_2 and the mixed oxides of Cu_2O and SiO_2 rich in SiO_2 or even the formation of continuous scale of SiO_2, so the outward diffusion of Cu is blocked effectively. This is beneficial to improve the high-temperature oxidation resistance of Cu-Si alloys, so this effect can be regarded as positive impact. Second, grain refining enhances the effective-diffusion coefficient of each component of the Cu-Si alloy and oxygen, so oxides form quickly, which makes the mass gain of the alloy also increase quickly. This is harmful to improve the high-temperature oxidation resistance of Cu-Si alloys, so this effect can be regarded as negative impact. Whether grain refining can improve the high-temperature oxidation resistance of Cu-Si alloys is determined by which of the two aspects mentioned above predominates. Comprehensively, for Cu-Si alloys, the positive impact predominates, so grain refining improves the high-temperature oxidation resistance of Cu-Si alloys.

5. CONCLUSIONS

The Cu-Si alloys with two compositions prepared by different techniques oxidized at 973 and 1073 K under 1 atm of flowing pure O_2 for 24 h formed similar complex scales like $CuO \rightarrow Cu_2O \rightarrow Cu_2O$ and SiO_2 (rich in SiO_2) $\rightarrow$ internal oxidation zone from outside to inside, and did not form continuous layers of SiO_2.

The oxidation rates of alloys prepared by MA were lower than those of the corresponding alloys prepared by CA subjected to the same treatment. The differences in oxidation rates are attributed to that the grain size reduction may enhance the diffusivity of Si, so the formation of mixed oxides of Cu_2O and SiO_2 rich in SiO_2 can be accelerated, which can effectively restrain the further formation of copper oxides. Grain refining improves the high-temperature oxidation resistance of Cu-Si alloys.

ACKNOWLEDGEMENTS

The authors are grateful to Dr. X. J. Zhang for his invaluable discussions and advice throughout this work. The work was financially supported by Program for Liaoning Excellent Talents in University (No. RC-05-15) and Liaoning Educational Committee (No. 20060683).

REFERENCES

1. S.W. Yang, H.Y. Chen, X.G. Zhu and Y. H. Wang, *Corrosion Science and Protection Technology* (Chinese), **19**, 5 (2007)
2. X. J. Zhang, S. Y. Wang, F. Gesmundo and Y. Niu, *Oxid. Met.*, **65**, 151 (2006)
3. D. Mukherjee, A. A. Khan, M. R. Kumar, S. Mukhejee, A. N. Alagappan, P. Nagarajan, A. S. Nesaraj, S. Ghosh and S. Muzhumathi, *Surf. Eng.*, **22**, 411 (2006)
4. S. L. Yang and F. H. Wang, *Oxid. Met.*, **65**, 195 (2006)
5. W. Wen, Y. Ping and F. H. Wang, *Surf. Coat. Technol.*, **201**, 7425 (2007)
6. S. L. Zhu, S. Cao, S. M. Li, C. G. Zhang, D. B. Xie, W. Wang, L. Xin and F. H. Wang, *Corrosion Science and Protection Technology* (Chinese), **20**, 86 (2008)
7. Z. Han, L. Lu, H. W. Zhang, Z. Q. Yang, F. H. Wang and K. Lu, *Oxid. Met.*, **63**, 261 (2005)
8. Y. Niu, S. Y. Wang and F. Gesmundo, *Oxid. Met.*, **65**, 285 (2006)
9. Z. Huang, X. Peng and F. Wang, *Oxid. Met.*, **65**, 223 (2006)
10. Z. H. Gan, Z. Y. Mao, F. C. Shen, J. Li and B. G. Ye, *Materials Science & Engineering* (Chinese), **15**, 50 (1997)
11. P. J. Ding, W. A. Lanford, S. Hymes and S. P.

Murarka, *Appl. Phys. Lett.*, **64**, 2897 (1994)
12. C. S. Hsu, H. Y. Hsieh and J. S. Fang, *J. Electron. Mater.*, **37**, 852 (2008)
13. Z. Q. Cao, W. H. Liu, G. P. Zhai and Y. Niu, *Trans Nonferrous Met Soc China*, **15**, 491 (2005)
14. S. V. Raj, *Oxid. Met.*, **70**, 85 (2008)
15. S. V. Raj, *Oxid. Met.*, **70**, 103 (2008)
16. K. X. Song, J. D. Xing, B. H. Tian, P. Liu and Q. M. Dong, *Journal of Wuhan University of Technology-Materials Science Edition*, **20**, 13 (2005)
17. K. X. Song, J. X. Gao, X. F. Xu, P. Q. Li, B. H. Tian and X. H. Guo, *Journal of Wuhan University of Technology-Materials Science Edition*, **22**, 22 (2007)
18. M. S. Li, *High Temperature Corrosion of Metal* (Chinese) Metallurgical Industry Press, Beijing (2001).
19. R. Z. Zhu, Y. D. He and H. B. Qi, *High-temperature Corrosion and High-temperature Resistant Materials* (Chinese) (Shanghai Sci & Tech Press, Shanghai (1995))
20. E. Arzt and E. Schultz, *New Materials by Mechanical Alloying Techniques* (Deutche Gesell Fur Metallkunde, Germany (1989))
21. R. Birringer, *Mater. Sci. Eng.* A, **117**, 33 (1989)
22. G. C. Hadjipanayis and R. W. Siegel, *Nanophase Materials, Synthesis, Properties, Application,* Kluwer Academic Publishers, London (1994).
23. J. Z. Jiang, C. Gente and R. Bormann, *Mater. Sci. Eng.* A, **242**, 268 (1998)
24. E. W. Hart, *Acta Metall.*, **5**, 597 (1957)
25. R. Herchl, N. N. Khoi, T. Homma and W. W. Smeltzer, *Oxid. Met.*, **4**, 35 (1972)
26. C. Suryanarayana, *Int. Mater. Rev.*, **40**, 41 (1995)
27. A. Atkinson, *Solid State Ionics*, **12**, 309 (1984)
28. F. H. Wang, *Oxid. Met.*, **48**, 215 (1997)
29. P. Kofstad, *High Temperature Corrosion of Metals*, Elsevier Science Publishing Co.,Inc., New York, (1988).